7724 J. Med. Chem. 2009, 52, 7724–7731
DOI: 10.1021/jm9007483

Journal of Medicinal Chemistry Article

Pentapeptides Displaying μ Opioid Receptor Agonist and δ Opioid Receptor Partial Agonist/Antagonist Properties†

Lauren C. Purington,‡ Irina D. Pogozheva,§ John R. Traynor,*,‡,∥ and Henry I. Mosberg*,§

‡Departments of Pharmacology and §Medicinal Chemistry, University of Michigan, Ann Arbor, Michigan, and ∥University of Michigan Substance Abuse Research Center, Ann Arbor, Michigan

Received May 29, 2009

Chronic use of μ-opioid agonists has been shown to cause neurochemical adaptations resulting in tolerance and dependence. While the analgesic effects of these drugs are mediated by μ-opioid receptors (MOR), several studies have shown that antagonism or knockdown of δ-opioid receptors (DOR) can lessen or prevent development of tolerance and dependence. On the basis of computational modeling of putative active and inactive conformations of MOR and DOR, we have synthesized a series of pentapeptides with the goal of developing a MOR agonist/DOR antagonist peptide with similar affinity at both receptors as a tool to probe functional opioid receptor interaction(s). The eight resulting naphthylalanine-substituted cyclic pentapeptides displayed variable mixed-efficacy profiles. The most promising peptide (**9**; Tyr-c(S−CH_2−S)[D-Cys-Phe-2-Nal-Cys]NH_2) displayed a MOR agonist and DOR partial agonist/antagonist profile and bound with equipotent affinity (K_i ∼ 0.5 nM) to both receptors, but also showed κ opioid receptor (KOR) agonist activity.

Introduction

Mu-opioid receptor (MOR[a]) agonists such as morphine are commonly used in the treatment of moderate to severe pain. However, use of such drugs is associated with side effects including the development of tolerance, limiting the usefulness of these compounds. It has been hypothesized that opioid compounds displaying MOR agonism paired with a selective δ- or κ-opioid receptor effect could lessen the severity of limiting side effects surrounding current MOR agonist use,[1] including respiratory depression and constipation as well as tolerance. In particular, studies pointing to a role of the δ opioid receptor (DOR) in modulating the development of MOR tolerance have led to the hypothesis that both MOR and DOR play major roles in the development of tolerance after chronic morphine exposure. For example, work in DOR knockout rodent models[2−4] or using DOR antagonists[5−8] was shown to prevent or lessen the severity of tolerance development to chronic morphine exposure. More recent in vivo work also points to a role of DOR in modulating morphine-induced behavioral sensitization and conditioned place preference in rodents.[9−11] It has been hypothesized that the formation of homo- or heterodimers of MOR and DOR leads to changes in their pharmacological behaviors including alteration in tolerance or dependence development.[6,12−14]

The growing body of evidence implicating a role of DOR in modulating MOR-induced tolerance suggests that opioid ligands with similar affinities at MOR and DOR but displaying agonism at MOR and antagonism at DOR might be of great clinical potential, especially for the treatment of chronic pain conditions. Consequently, many groups have developed compounds with MOR and DOR affinity, including peptidic[15−19] and nonpeptidic[20−24] ligands displaying MOR agonism and DOR antagonism. However, many of these compounds, while displaying the desired efficacy profile, do not have equivalent binding affinities to both MOR and DOR, thus limiting their usefulness in probing MOR−DOR interactions.

Our previous work led to the synthesis of peptide **1** (Tyr-c(S−CH_2−S)[D-Cys-Phe-Phe-Cys]NH_2).[25] Peptide **1** displayed a promising mixed-efficacy profile at MOR and DOR, binding with high affinity for both MOR and DOR while exhibiting full agonism at MOR and the κ opioid receptor (KOR) but only partial agonism at DOR. We wished

†This work is submitted in celebration of the 100th anniversary of the Division of Medicinal Chemistry.

*To whom correspondence should be addressed. For J.R.T.: phone, (734) 647-7479; fax, (734) 763-4450; E-mail: jtraynor@umich.edu; address, University of Michigan, 1150 W. Medical Center Drive, Ann Arbor MI 48109-5632.For H.I.M.: phone, (734) 764-8117; fax, (734) 763-5595; E-mail: him@umich.edu; address, University of Michigan, 428 Church Street, Ann Arbor MI 48109-1065.

[a] Abbreviations: Symbols and abbreviations are in accordance with recommendations of the IUPAC-IUB Joint Commission on Biochemical Nomenclature: Nomenclature and Symbolism for Amino Acids and Peptides. *Biochem. J.* **1984**, *219*, 345−373. All other abbreviations are as follows: 1-Nal, 3-(1-naphthyl)alanine; 2-Nal, 3-(2-naphthyl)alanine; AcOH, acetic acid; C_6-MOR, C_6 rat glioma cells stably expressing the μ-opioid receptor; C_6-DOR, C_6 rat glioma cells stably expressing the δ-opioid receptor; cAMP, cyclic adenosine monophosphate; CHO-KOR, Chinese hamster ovary cells stably expressing the κ-opioid receptor; DAMGO, [D-Ala^2,N-Me-Phe^4,Gly^5-ol]-enkephalin; DIEA, diisopropylethylamine; DMEM, Dulbecco's Modified Eagle Medium; DMF, dimethylformamide; DOR, δ opioid receptor; EXL, extracellular loop; Fmoc, 9-fluorenylmethyloxycarbonyl; FSK, forskolin; GPCR, G protein-coupled receptor; [^{35}S]GTPγS, [^{35}S]-guanosine-5′-O-(3-thio)triphosphate; HBTU, o-benzotriazole-N,N,N′,N′-tetramethyl-uronium-hexafluoro-phosphate; HOBT, 1-hydroxybenzotriazole; KOR, κ opioid receptor; MOR, μ opioid receptor; NTI, naltrindole; rmsd, root-mean-square deviation; RP-HPLC, reverse phase-high performance liquid chromatography; SNC80, 4-[(R)-[(2S,5R)-4-allyl-2,5-dimethylpiperazin-1-yl](3-methoxyphenyl)-methyl]-N,N-diethylbenzamide; TFA, trifluoroacetic acid; TM, transmembrane helixes; U69,593, (5α,7α,8β)-(−)-N-methyl-N-[7-(1-pyrrolidinyl)-1-oxaspiro[4,5]dec-8-yl]benzeneacetamide.

 Published on Web 09/29/2009

Table 1. Binding Affinities and Efficacies of Cyclic Opioid Pentapeptides **1**−**9** at MOR, DOR, and KOR[a]

			K_i (nM) ± SEM			efficacy (%) ± SEM		
peptide	sequence	linker	MOR	DOR	KOR	MOR	DOR	KOR
1	Tyr-c[D-Cys-Phe-Phe-Cys]NH_2	S−CH_2−S	0.016 ± 0.01	1.8 ± 0.8	2.5 ± 1.5	88 ± 1.1	45 ± 2.3	93 ± 3.4
2	Tyr-c[D-Cys-1-Nal-Phe-Cys]NH_2	S−S	0.08 ± 0.04	34 ± 4.5	21 ± 1.7	33 ± 1.6	0	59 ± 3.1
3	Tyr-c[D-Cys-1-Nal-Phe-Cys]NH_2	S−CH_2−S	0.33 ± 0.04	34 ± 0.7	5.8 ± 2.9	91 ± 4.5	23 ± 3.4	77 ± 6.3
4	Tyr-c[D-Cys-2-Nal-Phe-Cys]NH_2	S−S	0.72 ± 0.05	55 ± 0.3	145 ± 11	34 ± 1.5	0.7 ± 1.0	7.5 ± 2.1
5	Tyr-c[D-Cys-2-Nal-Phe-Cys]NH_2	S−CH_2−S	0.47 ± 0.2	15 ± 1.7	69 ± 0.6	34 ± 3.8	23 ± 1.6	35 ± 4.0
6	Tyr-c[D-Cys-Phe-1-Nal-Cys]NH_2	S−S	2.5 ± 0.9	7.1 ± 2.3	11 ± 1.8	88 ± 3.6	15 ± 1.5	100 ± 7.4
7	Tyr-c[D-Cys-Phe-1-Nal-Cys]NH_2	S−CH_2−S	0.61 ± 0.08	5.2 ± 0.4	6.0 ± 1.5	100 ± 3.8	22 ± 2.3	87 ± 2.4
8	Tyr-c[D-Cys-Phe-2-Nal-Cys]NH_2	S−S	1.2 ± 0.3	11 ± 6.4	5.9 ± 0.8	90 ± 1.4	2.0 ± 1.0	49 ± 3.6
9	Tyr-c[D-Cys-Phe-2-Nal-Cys]NH_2	S−CH_2−S	0.47 ± 0.2	0.48 ± 0.2	1.3 ± 0.4	99 ± 1.8	7.0 ± 2.3	89 ± 3.6

[a] 3-(1-Naphthyl)alanine and 3-(2-naphthyl)alanine substitution abbreviated as 1-Nal and 2-Nal, respectively. Cyclization abbreviated as S−S for disulfide linkage and S−CH_2−S for methylene dithioether linkage. Experiments were performed in C_6-MOR, C_6-DOR, or CHO-KOR cells. Binding affinities (K_i) were obtained by competitive displacement of radiolabeled [^{3}H]diprenorphine. Efficacy of pentapeptides at the three opioid receptors was determined using the [^{35}S]GTPγS binding assay. Efficacy is presented as percent of the maximal level of [^{35}S]GTPγS binding obtained with standard agonists for MOR, DOR, and KOR (DAMGO, SNC80, or U69,593, respectively) at a 10 μM concentration.

to improve peptide **1** by decreasing efficacy at DOR while increasing affinity for this receptor, retaining both efficacy and affinity at MOR, and reducing affinity at KOR. To pursue this aim, we examined the docking of **1** into computational models of MOR and DOR. On the basis of modeling of putative active and inactive conformations of MOR and DOR[26−29] and docking of **1** to these models, we focused on steric constraints surrounding the third and fourth Phe residues of **1**. We hypothesized that replacement of these Phe residues with bulkier side chains would decrease ligand affinity to the DOR active state but not the DOR inactive state and not affect binding to MOR, thus favoring the desired MOR agonist/DOR antagonist profile. Consequently, we designed eight analogues of peptide **1** containing naphthylalanine in place of Phe^3 or Phe^4 to more fully explore the steric limits of the receptor binding pocket at either of these positions. We have previously used naphthylalanine substitution to add steric bulk in cyclic peptides,[30] and this has been more recently applied to linear peptides.[31] In vitro, our cyclic peptides displayed variable MOR efficacies and had decreased DOR efficacy. One compound (peptide **9**; Tyr-c(S−CH_2−S)-[D-Cys-Phe-2-Nal-Cys]NH_2) displayed full agonism at MOR (99% stimulation compared with the full MOR agonist DAMGO) while acting as an antagonist at DOR in the [^{35}S]GTPγS assay, but with partial agonist activity in the adenylyl cyclase inhibition assay, and bound with similar subnanomolar affinity to MOR and DOR stably and independently expressed in C_6 rat glioma cells. Compound **9** also bound with high affinity to KOR and was an agonist at that receptor. Thus, incorporation of a substitution based on rational design and intended to highlight putative steric constraints resulted in a compound that had similar affinity for MOR and DOR but decreased DOR efficacy without compromising MOR agonism. This is an important step forward in the development of novel ligands presenting MOR agonist and DOR antagonist effects.

Results

Rationale for the Design of Pentapeptides Displaying MOR Agonism and DOR Antagonism. Previous work by our group led to the synthesis of the high-affinity, MOR-selective cyclic pentapeptide **1** (Tyr-c(S−CH_2−S)[D-Cys-Phe-Phe-Cys]-NH_2),[25] which has picomolar affinity for MOR (K_i = 0.016 nM) and nanomolar affinities for DOR (K_i = 1.8 nM) and KOR (K_i = 2.5 nM). When evaluated for efficacy at the three opioid receptors using the [^{35}S]GTPγS assay,[32] **1** displayed full agonism at MOR and KOR, but only partial agonism at DOR (Table 1). To understand the molecular mechanism underlying the mixed-efficacy profile of **1**, computational models of MOR and DOR were utilized. Peptide **1** was virtually docked in models of active and inactive conformations of MOR and DOR[26−29] (Figure 1) in a similar manner as MOR and DOR-selective tetrapeptides, JOM6 and JOM13, respectively, which were previously positioned in MOR and DOR models based on their structure−activity relationships and receptor mutagenesis data.[26,27,33,34] These active and inactive receptor models were designed based on the published crystal structure of the β_2-adrenergic receptor[35] (as described in the Experimental Section). Though the new adrenoreceptor-based models of opioid receptors differ from our previously published rhodopsin-based models[26,28,29,33] by some helix shifts and an outward movement of extracellular loop (EXL) 2 (rmsd in the range 2.3−2.6 Å for all Cα-atoms, excluding EXL2), the ligand binding mode and receptor−ligand interactions with residues from transmembrane helixes (TMs) 3, 5, 6, and 7 of either DOR or MOR remained essentially the same. Thus, we found that the docking mode of peptide ligands is more influenced by its interactions with helix residues than residues from EXL2, the modeling of which is expected to be less accurate.

Examination of the position of pentapeptide **1** inside the binding pocket of active and inactive MOR (Figure 1A,B) allowed us to obtain a low-energy conformation of **1** that did not have steric hindrances or other adverse interactions with residues in the receptor binding pocket in either receptor state. Peptide **1** docked in MOR showed favorable aromatic interactions between its Phe^3 side chain and the Trp^{318} side chain in TM7, which were more pronounced in the active conformation of MOR. These aromatic interactions may explain the preferential binding of **1** to MOR, as compared to DOR or KOR, which have Leu^{300} or Tyr^{312} at the corresponding position. The same conformation of **1**, when fitted into the active DOR model (Figure 1C), demonstrated some steric overlap between Phe^4 of the ligand and Trp^{284} from the TM6 of DOR, which was not observed in the inactive DOR model (Figure 1D). The docking of peptide **1** to both active and inactive conformations of MOR and its better compatibility with the inactive conformation of DOR is consistent with the MOR agonist/DOR partial agonist profile of **1**.

On the basis of the above, we hypothesized that incorporation of a bulkier naphthylalanine side chain in either the third or fourth position of pentapeptide **1** would affect its binding

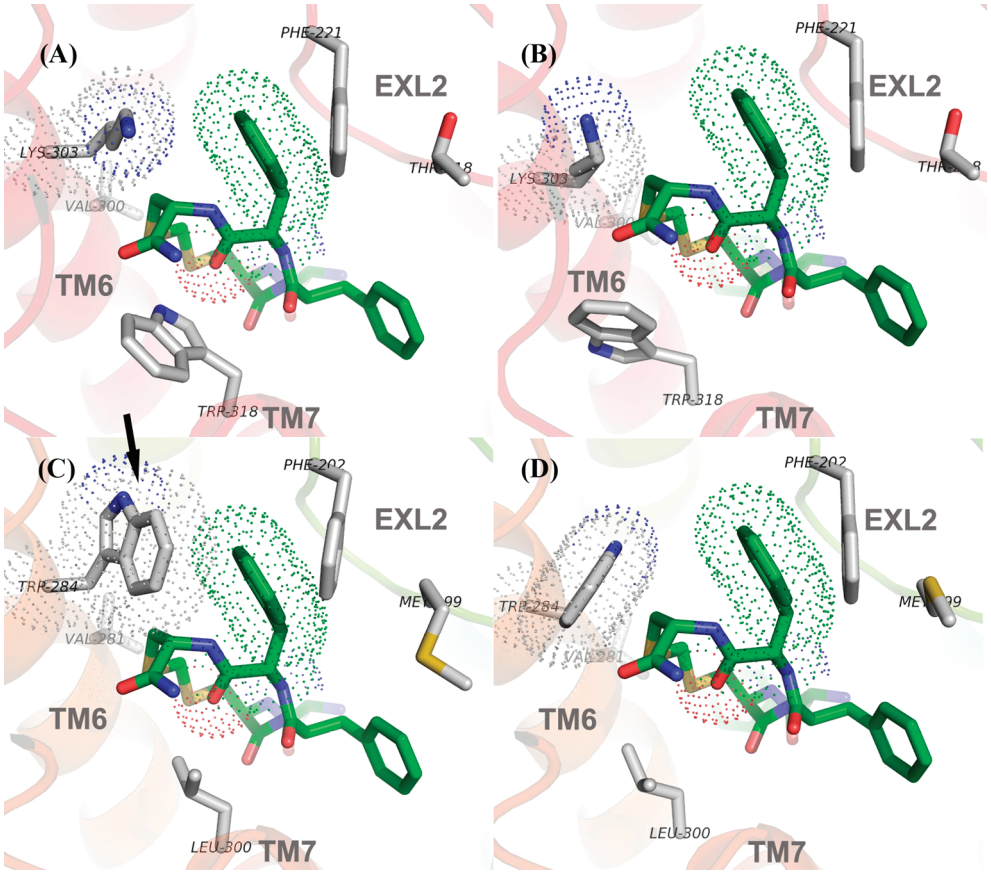

Figure 1. Modeling of peptide **1** in the binding pocket of putative active and inactive conformations of mouse MOR and human DOR. Peptide **1** docked in the putative active (A) and inactive (B) conformation of MOR shows no noticeable unfavorable interactions between ligand side chains and residues from the receptor binding pocket. Peptide **1** docked in the active conformation of DOR (C) shows a steric overlap of the peptide Phe^4 side chain with the side chain of receptor Trp^{284} from TM6 (arrow), while peptide **1** in the inactive conformation of DOR (D) does not show a similar steric hindrance.

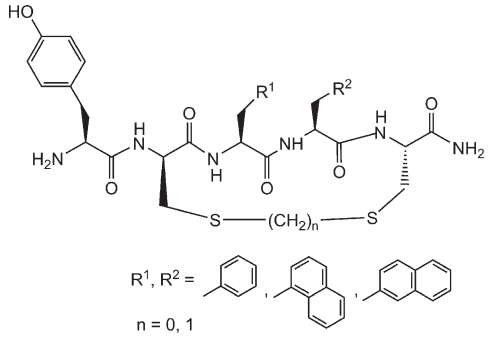

Figure 2. Naphthylalanine-containing analogues of peptide **1**.

and efficacy properties differentially at MOR and DOR and could result in potent MOR agonist/DOR antagonist ligands. To test this hypothesis, we replaced Phe^3 and Phe^4 of **1** with the bulkier 3-(1-naphthyl)alanine or 3-(2-naphthyl)-alanine (Figure 2) to provide eight new cyclic pentapeptides (**2**−**9**; Tables 1, 2). Peptides were cyclized via a disulfide bond (S−S) or methylene dithioether (S−CH_2−S) linkage to allow for altered size and flexibility of the cycle.

Analysis of Synthesized Pentapeptides 2−9 for Binding Affinity and Efficacy at Opioid Receptors. Most naphthylalanine peptides demonstrated relatively high binding affinities to MOR, DOR, and KOR as measured by competitive displacement of the radiolabeled nonselective opioid antagonist [^{3}H]diprenorphine. However, some loss in affinity to all three opioid receptors was generally noted as compared to the highly potent pentapeptide **1**. At MOR, the most significant loss of affinity occurred with peptide **6** ($p < 0.001$), while at DOR four peptides had ≥10-fold decreased affinity (**2**, **3**, **4** $p < 0.001$, and **5** $p < 0.05$). At KOR, peptides **4** and **5** had >10-fold decreased binding affinity when compared to **1** ($p < 0.001$) (Table 1). Of the eight peptides synthesized, only peptide **9** (Tyr-c(S−CH_2−S)[D-Cys-Phe-2-Nal-Cys]-NH_2) showed similar low nanomolar binding affinity to MOR, DOR, and KOR (K_i = 0.47, 0.48, and 1.3 nM, respectively).

Peptides **2**−**9** were also analyzed for efficacy at MOR, DOR, and KOR as determined by maximal stimulation of [^{35}S]GTPγS binding[32] as a percentage of 10 μM standard compounds DAMGO, SNC80, and U69,593 (Table 1). Peptides **3**, **6**, and **8** showed equivalent agonism at MOR as peptide **1** (~90% maximal stimulation), while peptides **2**, **4**, and **5** had decreased efficacy at MOR (31−34% stimulation; $p < 0.001$). In contrast, peptides **7** and **9** showed greater stimulation of [^{35}S]GTPγS binding at MOR than **1** ($p < 0.05$), displaying the same maximal stimulation. It is noteworthy that all peptides displaying decreased efficacy at MOR (**2**, **4**, and **5**) were substituted at position 3 with naphthylalanine. In contrast, analogues with naphthylalanine substitution at position 4 (**6**−**9**) showed equal or greater efficacy at MOR, indicating substitution at position 3 by residues with bulky side chains is deleterious for MOR agonism. One exception was peptide **3**, which has

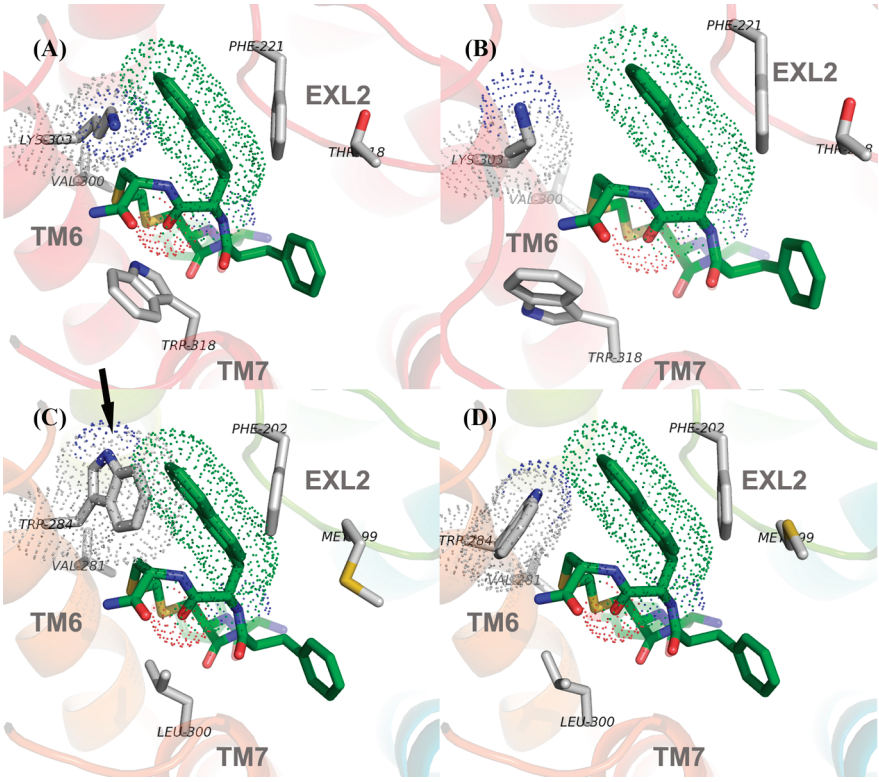

Figure 3. Pentapeptide **9** docked in the binding pocket of putative active and inactive conformations of mouse MOR and human DOR. The 2-naphthylalanine[4] side chain of peptide **9** shows minimal hindrance with receptor residue Lys[303] in the MOR active conformation (A) but an increased steric overlap with Trp[284] side chain (arrow) in the DOR active conformation (C). These hindrances are absent in the inactive conformations of both MOR (B) and DOR (D).

naphthylalanine substitution at position 3 and displayed high efficacy at MOR. Peptide **3** was cyclized via a methylene dithioether, possibly allowing greater flexibility of the peptide ring structure and leading to increased stimulation over the disulfide-cyclized counterpart **2**. At DOR, peptides **2**, **4**, **8**, and **9** behaved essentially as antagonists, providing very little or no [^{35}S]GTPγS stimulation. Compounds **3**, **5**, **6**, and **7** displayed partial agonism with maximal stimulation varying from 15 to 23%. The eight peptides displayed varying efficacy profiles at KOR, with most compounds behaving as partial to full agonists (maximal stimulation 35−100%).

Docking of Peptide 9 to Modeled MOR and DOR Active and Inactive Conformations. The binding and efficacy studies described above identify peptide **9** as a candidate ligand displaying the desired MOR agonism and DOR antagonism profile. To better understand the mechanism of the decreased efficacy of **9** at DOR, we docked this peptide in the modeled active and inactive conformations of MOR and DOR similar to the docking of peptide **1** (Figure 3).

The lowest energy conformation of peptide **9** exhibited no hindrance in the binding pocket of either active or inactive conformations of MOR (Figure 3A,B) nor in the inactive DOR conformation (Figure 3D). However, when compared to peptide **1** (Figure 2C), **9** shows greater overlap between its 2-naphthylalanine[4] and Trp[284] in the active conformation of DOR (Figure 3C). This reduced compatibility of **9** relative to **1** for the active state of DOR supports the decreased agonism at DOR. Modeling results also explain the high agonist efficacy of **9** at MOR, because **9** fits both receptor states well and may promote a conformational shift toward the active conformation of MOR where favorable aromatic interactions between Phe[3] and Trp[318] of MOR are more prominent.

Characterization of the Functional Properties of Peptide 9 at Opioid Receptors. In the [^{35}S]GTPγS binding assay, peptide **9** behaved as a full agonist at MOR with EC_{50} of 1.2 ± 0.05 nM (Figure 4A). On the other hand, at 10 μM concentration **9** produced only 7% of SNC80-induced stimulation of DOR-mediated [^{35}S]GTPγS binding (Table 1).

The properties of **9** were further evaluated by measuring its ability to inhibit SNC80-stimulated binding of [^{35}S]GTPγS to G-proteins. Peptide **9** produced a 3.1-fold rightward shift in the dose−response curve of SNC80 in C_6-DOR cells (Figure 4B); the EC_{50} for SNC80 was shifted from 75 ± 3.8 to 188 ± 31 nM in the presence of 100 nM **9** (p = 0.02). However, this shift and the calculated K_e value (48 ± 9.5 nM) for **9** was not consistent with its high binding affinity to DOR (K_i = 2.1 nM), indicating **9** may have some partial agonist efficacy at DOR which cannot be fully observed using the high efficacy-requiring [^{35}S]GTPγS binding assay. To more fully assess the extent of this partial agonism, we measured the ability of **9** to inhibit cAMP accumulation as a measure of adenylyl cyclase activity.[36] Because of downstream signaling amplification, it is easier to visualize partial agonism using this system. Peptide **9** was shown to be more potent (EC_{50}: 36 ± 4.8 nM) than SNC80 (EC_{50}: 166 ± 43 nM; p = 0.01) and behaved as a partial agonist, able to produce 55% inhibition of that seen with SNC80 (Figure 4C). The DOR-selective antagonist naltrindole (NTI) was without effect in this assay.

Discussion

The current studies were aimed toward the development of a potent compound with mixed MOR agonist/DOR antagonist properties, a profile that would be valuable to probe interactions of MOR and DOR and that has considerable

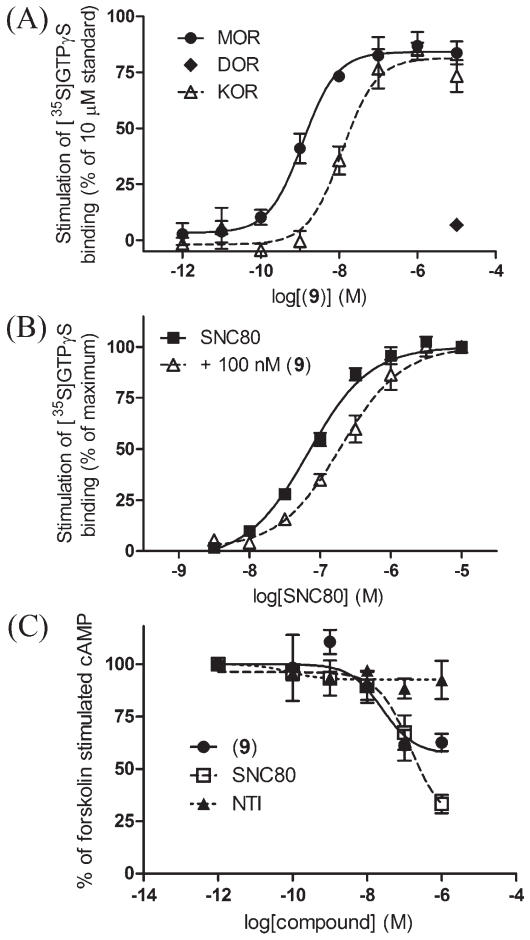

Figure 4. Pharmacological analysis of peptide **9**. (A) Activity of peptide **9** in the [^{35}S]GTPγS binding assay at MOR, DOR, and KOR. Results are plotted as percent stimulation compared to a 10 μM concentration of standard compounds (MOR standard agonist DAMGO, DOR standard agonist SNC80, and KOR standard agonist U69,593). Peptide **9** has 10-fold higher potency at MOR (EC_{50}: 1.2 $\pm$ 0.05 nM) than KOR (EC_{50}: 12 $\pm$ 0.1 nM) and 10 μM **9** produces only 6.9 $\pm$ 2.3% of SNC80-induced stimulation at DOR. (B) DOR antagonism of peptide **9** in the [^{35}S]GTPγS binding assay. Peptide **9** (100 nM) produces a 3.1-fold rightward shift in the SNC80 dose–response curve, indicating DOR antagonism. Calculated K_e = 48 $\pm$ 9.5 nM. Results are plotted as percentage of the maximum level of SNC80-stimulated [^{35}S]GTPγS binding. (C) Partial agonism of peptide **9** at DOR as illustrated by inhibition of adenylyl cyclase. Results are shown as percent inhibition of 5 μM forskolin-stimulated adenylyl cyclase production in C_6-DOR cells. Standard DOR agonist SNC80 (1 μM) gave 67 $\pm$ 4.4% inhibition of adenylyl cyclase production with a calculated maximal effect of 76 $\pm$ 8.8%, while 1 μM peptide **9** produced 37 $\pm$ 4.2% inhibition with a calculated maximum of 43 $\pm$ 9.0% inhibition. Peptide **9** is more potent (EC_{50} = 36 $\pm$ 4.8 nM) than SNC80 (EC_{50} = 166 $\pm$ 43 nM) in this assay. The DOR antagonist naltrindole (NTI) did not inhibit cAMP accumulation.

clinical promise. The eight newly synthesized cyclic pentapeptides represent modifications of our previously reported pentapeptide **1** (Tyr-c(S$-$CH$_2-$S)[D-Cys-Phe-Phe-Cys]NH$_2$),[25] which was characterized by high affinity binding to all opioid receptors and a mixed efficacy profile. On the basis of our computational modeling of active and inactive conformations of MOR and DOR and docking of **1** to these models (Figure 1), we focused on receptor–ligand interactions surrounding Phe^3 and Phe^4 residues of **1**. We designed several derivative peptides containing naphthylalanine substitution to more fully explore the steric limits of the receptor binding pocket at either of these positions. All peptides were evaluated for their potential to interact at both MOR and DOR via receptor binding and in vitro functional studies. The newly synthesized peptides demonstrated MOR agonism with variable efficacies and had greatly decreased DOR efficacy in the [^{35}S]GTPγS binding assay. One compound, peptide **9** (Tyr-c(S$-$CH$_2-$S)[D-Cys-Phe-2-Nal-Cys]NH$_2$), bound with similar subnanomolar affinity to MOR and DOR stably expressed in rat glioma cells and was characterized as an agonist at MOR and an antagonist or partial agonist at DOR depending on the assay used. This latter difference highlights the importance of the choice of assay in efficacy determination.[37]

The development of pentapeptide **9** represents a significant step forward in the development of a mixed-efficacy MOR agonist/DOR antagonist ligand. Previously reported mixed-efficacy ligands did not show the same equipotent affinity for both MOR and DOR[15–17,19–24] or the same full MOR agonist properties.[18,21,22] The results also represent a validation of our receptor models and a novel demonstration of the use of differences in modeled active and inactive states to design ligands with prescribed properties. In this example, steric differences in the binding site of the active and inactive DOR models were exploited by incorporating bulkier naphthylalanine in place of phenylalanine in residues 3 and 4 of lead peptide **1** to generate ligands with the desired MOR agonist/DOR antagonist profile.

Although peptide **9** displays the desired MOR/DOR mixed-efficacy profile, it also acts as a full agonist at KOR in the [^{35}S]GTPγS binding assay with EC_{50} of 12 $\pm$ 0.1 nM although it is 10-fold selective in potency for MOR over KOR (Figure 4A). This residual KOR activity is not surprising, as compound **1** was initially developed in a series aiming to improve KOR binding and efficacy.[25] Using computational models of KOR developed as described above for putative active and inactive conformation models of MOR and DOR, we are designing analogues that are intended to exhibit reduced KOR affinity while retaining the desired MOR agonist/DOR antagonist profile. Such compounds will allow us to characterize MOR and DOR interactions without the potential complication of concomitant KOR activation or antagonism.

Experimental Section

Materials. All Fmoc-protected amino acids were obtained from Advanced ChemTech (Louisville, KY) or Sigma-Aldrich (St. Louis, MO). All other reagents for peptide synthesis and characterization were from Sigma-Aldrich (St. Louis, MO) unless otherwise indicated. Fetal bovine serum and all cell culture media and additives were purchased from Gibco Life Sciences (Grand Island, NY). [D-Ala^2,*N*-Me-Phe^4,Gly^5-ol]-enkephalin (DAMGO) and all other biochemicals were obtained from Sigma-Aldrich and were of analytical grade. 4-[(*R*)-[(2*S*,5*R*)-4-allyl-2,5-dimethylpiperazin-1-yl](3-methoxyphenyl)-methyl]-*N*,*N*-diethylbenzamide (SNC80) was obtained from the Narcotic Drug and Opioid Peptide Basic Research Center at the University of Michigan (Ann Arbor, MI). [^{35}S]-guanosine-5′-*O*-(3-thio)triphosphate ([^{35}S]-GTPγS; 1250 Ci (46.2TBq)/mmol) and [^{3}H]-diprenorphine were purchased from Perkin-Elmer (Boston, MA). Cyclic AMP accumulation was determined by radioimmunoassay (GE Healthcare, Piscataway, NJ).

Structural Modeling. The homology modeling of the inactive conformation of human DOR (residues 45–338, UniProt accession code P41143) and mouse MOR (residues 64–354, UniProt accession code P42866) was performed as previously

described[26,27,38] using the more recent structure of the β2-adrenergic receptor fused with T4 lysozyme (PDB code 2rh1).[35] Distance geometry calculations with DIANA[39] were used to provide helix shift and loop modeling. To model the active receptor conformation, we included several structural constraints between TM 3, 5, and 6 that have been shown to be compatible with active states of different GPCRs.[27] Introduction of these constraints allowed us to reproduce the significant movement of TM6 that has been suggested based on numerous experimental studies of different GPCRs, as well as on the comparison of the rhodopsin (1f88)[40] and opsin (3dqb)[41] crystal structures.

3D structures of cyclic pentapeptides were generated by QUANTA (Accelrys Inc.) using residue substitution of previously modeled pentapeptides[25] followed by molecular mechanics computations using the CHARMm force field. Several conformations of disulfide or methylene dithioether bridges and different rotamers of residues in the third and fourth positions of pentapeptides were tested during ligand docking. Several low energy conformations (within 2 kcal/mol) were manually positioned inside the receptor binding cavity similarly to tetrapeptides JOM6 and JOM13, whose docking in DOR and MOR has been previously justified using conformational and mutagenesis analysis.[26,27,33,34] During ligand docking, we selected those low energy conformations that better satisfied the following criteria: (1) provided interactions between Tyr^1 and Phe^3 and functionally important receptor residues (Asp^{147} from TM3, His^{297} from TM6, and Trp^{318} from TM7 of MOR[27] or corresponding Asp^{128}, His^{278}, and Leu^{300} in DOR), (2) had minimal steric overlap, and (3) formed more hydrogen-bonds between receptor and ligand polar groups. The docking pose of each ligand was subsequently refined using the solid docking module of QUANTA. The opioid receptor models are available upon request.

Solid Phase Peptide Synthesis. All peptides were synthesized by solid phase methods[42] on an ABI model 431A solid phase peptide synthesizer (Applied Biosystems, Foster City, CA) as previously published.[25] Rink resin (Advanced ChemTech) was used as the solid support for C-terminal carboxamide peptides. Peptide elongation on the peptide-resin involved treating resin with piperidine (Sigma-Aldrich) to cleave the Fmoc-protecting group, diisopropylethylamine (DIEA) activation, followed by coupling of the next amino acid with *o*-benzotriazol-1-yl-*N*,*N*,*N*′,*N*′-tetramethyl uronium hexafluorophosphate (HBTU) and 1-hydroxybenzotriazole (HOBt, Applied Biosystems). These steps were repeated until the entire peptide was assembled. A solution of trifluoroacetic acid/H_2O/tri-isopropylsilane (9:0.5:0.5, v/v/v) was used to cleave the linear peptide from the resin and simultaneously remove the side chain-protecting groups. The peptide solution was filtered from the resin and then subjected to semipreparative reverse phase high-performance liquid chromatography (RP-HPLC) to afford the linear disulfhydryl-containing peptide.

General Method for Disulfide Cyclization of Peptides. To obtain disulfide-cyclized peptides, linear disulfhydryl-containing peptide was dissolved in a 1% (v/v) acetic acid (AcOH) in H_2O solution (saturated with N_2) at 5 °C (1 mg linear peptide/mL of aqueous AcOH solution). The pH of the peptide solution was raised to 8.5 using NH_4OH, followed by the addition of 4 equiv of $K_3Fe(CN)_6$. The reaction mixture was stirred for 2 min and quenched by adjusting the pH to 3.5 with AcOH. The mixture was then subjected to semipreparative RP-HPLC to afford the disulfide-cyclized peptide.

General Method for Methylene Dithioether Cyclization of Peptides. To form methylene dithioether-containing cyclic peptides, linear disulfhydryl peptide was added to dimethylformamide (DMF) and maintained at 5 °C under a N_2 atmosphere (0.1 mg linear peptide/mL DMF). Approximately 10 equiv of potassium *t*-butoxide was added to the peptide solution, followed by the addition of 10 equiv of dibromomethane. The reaction was quenched with 5 mL AcOH after 2 h and the solvent removed in vacuo. The residue was dissolved in water, filtered, and subjected to semipreparative RP-HPLC to obtain the methylene dithioether cyclized peptide.

Table 2. Analytical Data for Peptides **2**−**9**

	MW[a]		HPLC (min; R_t)[b]	
peptide	calcd (MW)	obsd (MW + 1)	system A	system B
2	728.2	729.237	35.23	31.97
3	742.3	743.260	35.13	31.60
4	728.2	729.241	35.71	32.14
5	742.3	743.260	35.81	32.18
6	728.2	729.238	35.88	33.22
7	742.3	743.255	35.79	32.71
8	728.2	729.248	35.85	32.84
9	742.3	743.265	35.92	33.09

[a] Observed molecular weights determined by high resolution mass spectrometry (HRMS). [b] Retention time assessed by analytical high-performance liquid chromatography (HPLC) using two solvent systems; (A) 0.1% trifluoroacetic acid (TFA) in water (w/v)/0.1% TFA in acetonitrile with a gradient of 0−70% organic component in 70 min and (B) 0.1% TFA in water/0.1% TFA in methanol with a gradient of 20−70% organic component in 50 min, monitored at 230 nm, samples in H_2O with 0.1% TFA (elution column heated at 35 °C). All peptides had >97% purity determined by HPLC.

Characterization of Peptides. All final product peptides were >97% pure as assessed by analytical RP-HPLC on a Vydac 218TP C-18 column (The Nest Group, Southboro, MA) using two solvent systems: (A) 0.1% trifluoroacetic acid (TFA, w/v) in water/0.1% TFA (w/v) in acetonitrile with a gradient of 0−70% organic component in 70 min and (B) 0.1% TFA (w/v) in water/0.1% TFA (w/v) in methanol with a gradient of 20−70% organic component in 50 min, monitored at 230 nm. All peptides displayed the appropriate molecular weights as determined by high resolution mass spectroscopy (HRMS; Table 2) (Protein Structure facility, University of Michigan, Ann Arbor, MI).

Cell Lines and Membrane Preparations. C_6-rat glioma cells stably transfected with a rat μ (C_6-MOR) or rat δ (C_6-DOR) opioid receptor[43] and Chinese hamster ovary (CHO) cells stably expressing a human κ (CHO-KOR) opioid receptor[44] were used. Cells were grown to confluence at 37 °C in 5% CO_2 in either Dulbecco's Modified Eagle's Medium (DMEM, C_6 cells), or DMEM-F12 medium (CHO-κ) containing 10% fetal bovine serum. To prepare membranes for biochemical assays as described previously,[45] confluent cells were washed twice with ice-cold phosphate-buffered saline (0.9% NaCl, 0.61 mM Na_2HPO_4, and 0.38 mM KH_2PO_4, pH 7.4), detached from the plates by incubation in harvesting buffer (20 mM HEPES, pH 7.4, 150 mM NaCl, and 0.68 mM EDTA) at room temperature, and pelleted by centrifugation at 200*g* for 3 min. The cell pellet was suspended in ice-cold 50 mM Tris-HCl buffer, pH 7.4, and homogenized with a Tissue Tearor (Biospec Products, Inc., Bartlesville, OK) for 20 s at setting 4. The homogenate was centrifuged at 20000*g* for 20 min at 4 °C and the pellet rehomogenized in 50 mM Tris-HCl with a Tissue Tearor for 10 s at setting 2, followed by recentrifugation. The final pellet was resuspended in 50 mM Tris-HCl, to 0.5−1.0 mg/mL protein and frozen in aliquots at −80 °C. Protein concentration was determined using the BCA protein assay[46] (Thermo Fisher Scientific, Rockford, IL) using bovine serum albumin as the standard.

Radioligand Binding Assays. Opioid ligand-binding assays were based on the competitive displacement of [^{3}H]diprenorphine by the test compound from membrane preparations containing opioid receptors as described above.[25] The assay mixture, containing membrane suspension (10−20 μg protein/tube) in 50 mM Tris-HCl buffer (pH 7.4), [^{3}H]diprenorphine (0.2 nM), and increasing concentrations of test peptide, was incubated at 25 °C for 1 h to allow binding to reach equilibrium. Subsequently, the samples were filtered rapidly through GF/C

filters (Whatman, Middlesex, UK) using a Brandel harvester and washed three times with ice-cold 50 mM Tris-HCl buffer. The radioactivity retained on dried filters was determined by liquid scintillation counting after saturation with EcoLume liquid scintillation cocktail (MP Biomedicals, Solon, OH) in a Wallac 1450 MicroBeta (PerkinElmer, Waltham, MA). Nonspecific binding was determined using 10 μM naloxone. K_i values were determined from nonlinear regression analysis to fit a logistic equation to the competition data using GraphPad Prism 5.01 software (GraphPad Software, La Jolla, CA). The results presented are the mean from at least three separate assays, each performed in duplicate.

[^{35}S]GTPγS Binding Assay. Agonist stimulation of [^{35}S]-GTPγS binding was measured as described previously.[32] Briefly, membranes (20−30 μg of protein/tube) were incubated in GTPγS binding buffer (50 mM Tris-HCl, pH 7.4, 100 mM NaCl, and 5 mM $MgCl_2$) containing 0.1 nM [^{35}S]GTPγS, 100 μM GDP, and varying concentrations (0.001−10000 nM) or a maximum concentration (10 μM) of opioid peptides, compared with standards DAMGO, SNC80, or U69,593 (10 μM) in a total volume of 500 μL for 1 h at 25 °C. The reaction was terminated by rapidly filtering through GF/C filters and washing four times with 2 mL of ice-cold GTPγS binding buffer. Retained radioactivity was measured as described in radioligand binding assay methods. Experiments were performed at least three times in duplicate. EC_{50} values were determined by nonlinear regression analysis using GraphPad Prism 5.01 software as described above. To determine antagonism of **9**, [^{35}S]GTPγS binding was determined for SNC80 in the presence or absence of 100 nM **9**. The IC_{50} value in the presence of 100 nM **9** was divided by the IC_{50} value for SNC80 alone, and this ratio (DR) was employed to calculate the K_e value using the equation K_e = [antagonist]/(DR-1).

Whole Cell Acute Inhibition of Adenylyl Cyclase. Inhibition of adenylyl cyclase by opioid standards or test peptides was measured in C_6-DOR cells grown to confluence in 24-well plates.[36] Cells were washed in serum-free DMEM at least 30 min prior to the start of the assay and incubated with vehicle or various concentrations (0.1−1000 nM) of SNC80, naltrindole, or peptide **9** in serum-free media containing 5 μM forskolin (FSK) and 1 mM 3-isobutyl-1-methylxanthine for 10 min at 37 °C. The assay was quenched by replacing media with 1 mL ice-cold 3% perchloric acid and 30 min incubation at 4 °C. A 400 μL aliquot of sample was neutralized with 2.5 M $KHCO_3$ and centrifuged 1 min at 11000*g*. Cyclic AMP (cAMP) was measured from the supernatant using a radioimmunoassay kit from GE Healthcare (Piscataway, NJ) according to the manufacturer's instructions. Inhibition of cAMP accumulation by **9** or standard opioid ligands was calculated as a percent of FSK-stimulated cAMP accumulation in vehicle-treated cells. EC_{50} values were calculated for each compound using GraphPad Prism 5.01 software. Experiments were performed in duplicate and repeated a minimum of three times.

Statistical Analysis. Data were analyzed using Student's two-tailed *t* test or a one-way analysis of variance followed by Bonferroni's posthoc test using GraphPad Prism version 5.01 for Windows (GraphPad Software, San Diego, CA www.graphpad.com). *p* values less than 0.05 were considered to be significant.

Acknowledgment. This work was funded by NIH grants DA04087 (J.R.T.) and DA03910 (H.I.M.). L.C.P. was supported by DA007281 and DA007267. We thank Hui-Fang Song for technical assistance with the [^{3}H]diprenorphine binding assays and Jessica Anand for assistance with the HRMS analyses.

References

(1) Schiller, P. W. Bi- or multifunctional opioid peptide drugs. *Life Sci.* **2009**, in press. DOI: 10.1016/j.lfs.2009.020.025.

(2) Kest, B.; Lee, C. E.; McLemore, G. L.; Inturrisi, C. E. An antisense oligodeoxynucleotide to the delta opioid receptor (DOR-1) inhibits morphine tolerance and acute dependence in mice. *Brain Res. Bull.* **1996**, *39*, 185–188.

(3) Nitsche, J. F.; Schuller, A. G.; King, M. A.; Zengh, M.; Pasternak, G. W.; Pintar, J. E. Genetic dissociation of opiate tolerance and physical dependence in delta-opioid receptor-1 and preproenkephalin knock-out mice. *J. Neurosci.* **2002**, *22*, 10906–10913.

(4) Zhu, Y.; King, M. A.; Schuller, A. G.; Nitsche, J. F.; Reidl, M.; Elde, R. P.; Unterwald, E.; Pasternak, G. W.; Pintar, J. E. Retention of supraspinal delta-like analgesia and loss of morphine tolerance in delta opioid receptor knockout mice. *Neuron* **1999**, *24*, 243–252.

(5) Abdelhamid, E. E.; Sultana, M.; Portoghese, P. S.; Takemori, A. E. Selective blockage of delta opioid receptors prevents the development of morphine tolerance and dependence in mice. *J. Pharmacol. Exp. Ther.* **1991**, *258*, 299–303.

(6) Daniels, D. J.; Lenard, N. R.; Etienne, C. L.; Law, P. Y.; Roerig, S. C.; Portoghese, P. S. Opioid-induced tolerance and dependence in mice is modulated by the distance between pharmacophores in a bivalent ligand series. *Proc. Natl. Acad. Sci. U.S.A* **2005**, *102*, 19208–19213.

(7) Fundytus, M. E.; Schiller, P. W.; Shapiro, M.; Weltrowska, G.; Coderre, T. J. Attenuation of morphine tolerance and dependence with the highly selective delta-opioid receptor antagonist TIPP[Ψ]. *Eur. J. Pharmacol.* **1995**, *286*, 105–108.

(8) Hepburn, M. J.; Little, P. J.; Gingras, J.; Kuhn, C. M. Differential effects of naltrindole on morphine-induced tolerance and physical dependence in rats. *J. Pharmacol. Exp. Ther.* **1997**, *281*, 1350–1356.

(9) Chefer, V. I.; Shippenberg, T. S. Augmentation of Morphine-Induced Sensitization but Reduction in Morphine Tolerance and Reward in Delta-Opioid Receptor Knockout Mice. *Neuropsychopharmacology* **2009**, *34*, 887–898.

(10) Shippenberg, T. S.; Chefer, V. I.; Thompson, A. C. Delta-opioid receptor antagonists prevent sensitization to the conditioned rewarding effects of morphine. *Biol. Psychiatry* **2009**, *65*, 169–174.

(11) Timar, J.; Gyarmati, Z.; Furst, Z. The development of tolerance to locomotor effects of morphine and the effect of various opioid receptor antagonists in rats chronically treated with morphine. *Brain Res. Bull.* **2005**, *64*, 417–424.

(12) George, S. R.; Fan, T.; Xie, Z.; Tse, R.; Tam, V.; Varghese, G.; O'Dowd, B. F. Oligomerization of mu- and delta-opioid receptors. Generation of novel functional properties. *J. Biol. Chem.* **2000**, *275*, 26128–26135.

(13) Gomes, I.; Gupta, A.; Filipovska, J.; Szeto, H. H.; Pintar, J. E.; Devi, L. A. A role for heterodimerization of mu and delta opiate receptors in enhancing morphine analgesia. *Proc. Natl. Acad. Sci. U.S.A* **2004**, *101*, 5135–5139.

(14) Rozenfeld, R.; Abul-Husn, N. S.; Gomez, I.; Devi, L. A. An emerging role for the delta opioid receptor in the regulation of mu opioid receptor function. *Sci. World J.* **2007**, *7*, 64–73.

(15) Balboni, G.; Guerrini, R.; Salvadori, S.; Bianchi, C.; Rizzi, D.; Bryant, S. D.; Lazarus, L. H. Evaluation of the Dmt-Tic pharmacophore: conversion of a potent delta-opioid receptor antagonist into a potent delta agonist and ligands with mixed properties. *J. Med. Chem.* **2002**, *45*, 713–720.

(16) Balboni, G.; Salvadori, S.; Guerrini, R.; Negri, L.; Giannini, E.; Jinsmaa, Y.; Bryant, S. D.; Lazarus, L. H. Potent delta-opioid receptor agonists containing the Dmt-Tic pharmacophore. *J. Med. Chem.* **2002**, *45*, 5556–5563.

(17) Salvadori, S.; Guerrini, R.; Balboni, G.; Bianchi, C.; Bryant, S. D.; Cooper, P. S.; Lazarus, L. H. Further studies on the Dmt-Tic pharmacophore: hydrophobic substituents at the C-terminus endow delta antagonists to manifest mu agonism or mu antagonism. *J. Med. Chem.* **1999**, *42*, 5010–5019.

(18) Schiller, P. W.; Fundytus, M. E.; Merovitz, L.; Weltrowska, G.; Nguyen, T. M.; Lemieux, C.; Chung, N. N.; Coderre, T. J. The opioid mu agonist/delta antagonist DIPP-NH(2)[Ψ] produces a potent analgesic effect, no physical dependence, and less tolerance than morphine in rats. *J. Med. Chem.* **1999**, *42*, 3520–3526.

(19) Yamamoto, T.; Nair, P.; Vagner, J.; Largent-Milnes, T.; Davis, P.; Ma, S. W.; Navratilova, E.; Moye, S.; Tumati, S.; Lai, J.; Yamamura, H. I.; Vanderah, T. W.; Porreca, F.; Hruby, V. J. A Structure−Activity Relationship Study and Combinatorial Synthetic Approach of C-Terminal Modified Bifunctional Peptides that are delta/mu Opioid Receptor Agonists and Neurokinin 1 Receptor Antagonists. *J. Med. Chem.* **2008**, *51*, 1369–1376.

(20) Ananthan, S.; Johnson, C. A.; Carter, R. L.; Clayton, S. D.; Rice, K. C.; Xu, H.; Davis, P.; Porreca, F.; Rothman, R. B. Synthesis, opioid receptor binding, and bioassay of naltrindole analogues substituted in the indolic benzene moiety. *J. Med. Chem.* **1998**, *41*, 2872–2881.

(21) Ananthan, S.; Kezar, H. S., III; Carter, R. L.; Saini, S. K.; Rice, K. C.; Wells, J. L.; Davis, P.; Xu, H.; Dersch, C. M.; Bilsky, E. J.; Porreca, F.; Rothman, R. B. Synthesis, opioid receptor binding, and biological activities of naltrexone-derived pyrido- and pyrimidomorphinans. *J. Med. Chem.* **1999**, *42*, 3527–3538.
(22) Ananthan, S.; Khare, N. K.; Saini, S. K.; Seitz, L. E.; Bartlett, J. L.; Davis, P.; Dersch, C. M.; Porreca, F.; Rothman, R. B.; Bilsky, E. J. Identification of opioid ligands possessing mixed mu agonist/delta antagonist activity among pyridomorphinans derived from naloxone, oxymorphone, and hydromorphone. *J. Med. Chem.* **2004**, *47*, 1400–1412.
(23) Cheng, K.; Kim, I. J.; Lee, M. J.; Adah, S. A.; Raymond, T. J.; Bilsky, E. J.; Aceto, M. D.; May, E. L.; Harris, L. S.; Coop, A.; Dersch, C. M.; Rothman, R. B.; Jacobson, A. E.; Rice, K. C. Opioid ligands with mixed properties from substituted enantiomeric *N*-phenethyl-5-phenylmorphans. Synthesis of a mu-agonist delta-antagonist and delta-inverse agonists. *Org. Biomol. Chem.* **2007**, *5*, 1177–1190.
(24) Hiebel, A. C.; Lee, Y. S.; Bilsky, E.; Giuvelis, D.; Deschamps, J. R.; Parrish, D. A.; Aceto, M. D.; May, E. L.; Harris, L. S.; Coop, A.; Dersch, C. M.; Partilla, J. S.; Rothman, R. B.; Cheng, K.; Jacobson, A. E.; Rice, K. C. Probes for narcotic receptor mediated phenomena. 34. Synthesis and structure−activity relationships of a potent mu-agonist delta-antagonist and an exceedingly potent antinociceptive in the enantiomeric C9-substituted 5-(3-hydroxyphenyl)-*N*-phenylethylmorphan series. *J. Med. Chem.* **2007**, *50*, 3765–3776.
(25) Przydzial, M. J.; Pogozheva, I. D.; Ho, J. C.; Bosse, K. E.; Sawyer, E.; Traynor, J. R.; Mosberg, H. I. Design of high affinity cyclic pentapeptide ligands for kappa-opioid receptors. *J. Pept. Res.* **2005**, *66*, 255–262.
(26) Fowler, C. B.; Pogozheva, I. D.; LeVine, H., III; Mosberg, H. I. Refinement of a homology model of the mu-opioid receptor using distance constraints from intrinsic and engineered zinc-binding sites. *Biochemistry* **2004**, *43*, 8700–8710.
(27) Fowler, C. B.; Pogozheva, I. D.; Lomize, A. L.; LeVine, H., III; Mosberg, H. I. Complex of an active mu-opioid receptor with a cyclic peptide agonist modeled from experimental constraints. *Biochemistry* **2004**, *43*, 15796–15810.
(28) Pogozheva, I. D.; Lomize, A. L.; Mosberg, H. I. The transmembrane 7-alpha-bundle of rhodopsin: distance geometry calculations with hydrogen bonding constraints. *Biophys. J.* **1997**, *72*, 1963–1985.
(29) Pogozheva, I. D.; Lomize, A. L.; Mosberg, H. I. Opioid receptor three-dimensional structures from distance geometry calculations with hydrogen bonding constraints. *Biophys. J.* **1998**, *75*, 612–634.
(30) Heyl, D. L.; Mosberg, H. I. Modification of the Phe3 aromatic moiety in delta receptor-selective dermorphin/deltorphin-related tetrapeptides. Effects on opioid receptor binding. *Int. J. Pept. Protein Res.* **1992**, *39*, 450–457.
(31) Fichna, J.; do-Rego, J. C.; Janecki, T.; Staniszewska, R.; Poels, J.; Broeck, J. V.; Costentin, J.; Schiller, P. W.; Janecka, A. Novel highly potent mu-opioid receptor antagonist based on endomorphin-2 structure. *Bioorg. Med. Chem. Lett.* **2008**, *18*, 1350–1353.
(32) Traynor, J. R.; Nahorski, S. R. Modulation by mu-opioid agonists of guanosine-5′-*O*-(3-[^{35}S]thio)triphosphate binding to membranes from human neuroblastoma SH-SY5Y cells. *Mol. Pharmacol.* **1995**, *47*, 848–854.
(33) Mosberg, H. I.; Fowler, C. B. Development and validation of opioid ligand−receptor interaction models: the structural basis of mu vs delta selectivity. *J. Pept. Res.* **2002**, *60*, 329–335.
(34) Pogozheva, I. D.; Przydzial, M. J.; Mosberg, H. I. Homology modeling of opioid receptor−ligand complexes using experimental constraints. *AAPS J.* **2005**, *7*, E434–448.
(35) Rasmussen, S. G.; Choi, H. J.; Rosenbaum, D. M.; Kobilka, T. S.; Thian, F. S.; Edwards, P. C.; Burghammer, M.; Ratnala, V. R.; Sanishvili, R.; Fischetti, R. F.; Schertler, G. F.; Weis, W. I.; Kobilka, B. K. Crystal structure of the human beta2 adrenergic G-protein-coupled receptor. *Nature* **2007**, *450*, 383–387.
(36) Clark, M. J.; Neubig, R. R.; Traynor, J. R. Endogenous regulator of G protein signaling proteins suppress Galphao-dependent, mu-opioid agonist-mediated adenylyl cyclase supersensitization. *J. Pharmacol. Exp. Ther.* **2004**, *310*, 215–222.
(37) Nieland, N. P.; Moynihan, H. A.; Carrington, S.; Broadbear, J.; Woods, J. H.; Traynor, J. R.; Husbands, S. M.; Lewis, J. W. Structural determinants of opioid activity in derivatives of 14-aminomorphinones: effect of substitution in the aromatic ring of cinnamoylaminomorphinones and codeinones. *J. Med. Chem.* **2006**, *49*, 5333–5338.
(38) Przydzial, M. J.; Pogozheva, I. D.; Bosse, K. E.; Andrews, S. M.; Tharp, T. A.; Traynor, J. R.; Mosberg, H. I. Roles of residues 3 and 4 in cyclic tetrapeptide ligand recognition by the kappa-opioid receptor. *J. Pept. Res.* **2005**, *65*, 333–342.
(39) Guntert, P.; Wuthrich, K. Improved efficiency of protein structure calculations from NMR data using the program DIANA with redundant dihedral angle constraints. *J. Biomol. NMR* **1991**, *1*, 447–456.
(40) Palczewski, K.; Kumasaka, T.; Hori, T.; Behnke, C. A.; Motoshima, H.; Fox, B. A.; Le Trong, I.; Teller, D. C.; Okada, T.; Stenkamp, R. E.; Yamamoto, M.; Miyano, M. Crystal structure of rhodopsin: A G protein-coupled receptor. *Science* **2000**, *289*, 739–745.
(41) Scheerer, P.; Park, J. H.; Hildebrand, P. W.; Kim, Y. J.; Krauss, N.; Choe, H. W.; Hofmann, K. P.; Ernst, O. P. Crystal structure of opsin in its G-protein-interacting conformation. *Nature* **2008**, *455*, 497–502.
(42) Stewart, J. M., Young, J. D. *Solid-Phase Peptide Synthesis*, 2 ed.; Pierce Chemical Company: Rockford, IL, 1984.
(43) Lee, K. O.; Akil, H.; Woods, J. H.; Traynor, J. R. Differential binding properties of oripavines at cloned mu- and delta-opioid receptors. *Eur. J. Pharmacol.* **1999**, *378*, 323–330.
(44) Husbands, S. M.; Neilan, C. L.; Broadbear, J.; Grundt, P.; Breeden, S.; Aceto, M. D.; Woods, J. H.; Lewis, J. W.; Traynor, J. R. BU74, a complex oripavine derivative with potent kappa opioid receptor agonism and delayed opioid antagonism. *Eur. J. Pharmacol.* **2005**, *509*, 117–125.
(45) Clark, M. J.; Harrison, C.; Zhong, H.; Neubig, R. R.; Traynor, J. R. Endogenous RGS protein action modulates mu-opioid signaling through Galphao. Effects on adenylyl cyclase, extracellular signal-regulated kinases, and intracellular calcium pathways. *J. Biol. Chem.* **2003**, *278*, 9418–9425.
(46) Smith, P. K.; Krohn, R. I.; Hermanson, G. T.; Mallia, A. K.; Gartner, F. H.; Provenzano, M. D.; Fujimoto, E. K.; Goeke, N. M.; Olson, B. J.; Klenk, D. C. Measurement of protein using bicinchoninic acid. *Anal. Biochem.* **1985**, *150*, 76–85.